Received: 4 June 2020 | Revised: 10 August 2020 | Accepted: 27 August 2020

DOI: 10.1002/ar.24546

FULL LENGTH ARTICLE

The Anatomical Record | WILEY

Ultrastructure of eggshell and embryological development of *Salvator merianae* (Squamata: Teiidae)

María Belén Arrieta[1] | **Gabriela Beatriz Olea**[2] | **Florencia Evelyn Rodríguez**[2] | **Daniel Marcelo Lombardo**[3]

[1]Facultad de Ciencias Exactas y Naturales y Agrimensura, Universidad Nacional del Nordeste, Cátedra de Química Biológica, Corrientes, Argentina

[2]Facultad de Medicina, Laboratorio de Investigaciones Bioquímicas (LIBIM), Consejo Nacional de Investigaciones Científicas y Técnicas (CONICET), Universidad Nacional del Nordeste, Corrientes, Argentina

[3]Facultad de Cs Veterinarias, Instituto de Investigación y Tecnología en Reproducción Animal (INITRA), Cátedra de Histología y Embriología, Universidad de Buenos Aires, Buenos Aires, Argentina

Correspondence
Daniel Marcelo Lombardo, Facultad de Cs Veterinarias, Instituto de Investigación y Tecnología en Reproducción Animal (INITRA), Universidad de Buenos Aires, Corrientes, Argentina.
Email: dmlombardo@gmail.com

Abstract

The objective of this study was to characterize the external morphology of *Salvator meriane* embryos in different stages of embryonic development and establish a relationship with the ultrastructure of the shell from oviductal transit to hatching. A total of 120 embryos were analyzed to describe their external morphology, and 78 eggs were used for the analysis of the shell. For embryonic development, the series was established according to the total length of the body. We established 40 embryonic stages from the primitive streak. In the early stages, the external morphological features are the C-shaped body, the maxillary, and mandibular fusion processes with the frontal process and the fusion of the forelimb with the digital plate. In the middle stages, the eyelid appears, and there are claws on the toes, cornification of fingers, and the onset of pigmentation. The last stage of embryonic development is characterized by the beginning of the formation of the scales, appear the toenails, and finalize the entire pigmentation. Regarding the relationship that exists with the ultrastructure of the egg during development, it was possible to observe a marked change in the composition of the shell and well-marked compaction during embryonic development, which may be related to the transport of calcium during embryonic ossification. Our results allowed us to show the complete sequence of embryonic development, determining the laying stage for this species. It was possible to establish a relationship with the ultrastructure of the eggshell from the oviductal transit to the moment of hatching.

KEYWORDS

eggshell, embryonic stage, lizard

1 | INTRODUCTION

The embryology of reptiles has been studied by several researchers (Kamal and Hammouda, 1965; Kamal et al., 1970; Parker 1879; Dufaure and Hubert, 1961). the first to do a normal pattern of the embryonic development of *Chelydra serpentina* was Yntema (1968). After that, the embryonic stages of other species of Testudines have been determined by Greenbaum and Carr (2002). The knowledge of normal embryogenesis is useful for allowing information on comparative and evolutionary anatomy, that may contribute to the descriptive or experimental research, Beggs et al., (2000), Hamburger and

María Belén Arrieta, and Gabriela Olea have contributed equally to this study.

Hamilton (1992), and Melo de Almeida et al., (2015), as well as it is useful as an instrument for ecological studies.

Developmental tables were done to several species (Boughner et al., 2007; Dufaure and Hubert 1961; Ferguson 1987; Greenbaum and Carr 2002; Lima et al., 2012; Olea and Sandoval, 2012; Py-Daniel et al., 2017; Renous-Lécuru et al., 1989; Rodríguez et al., 2018; Vieira et al., 2011; Yntema 1968). External morphological features are important to determine stages (Beggs et al., 2000; Hamburger and Hamilton 1992). For Sauropsida, Magnusson and Taylor (1980) were pioneers on the characterization of the embryonic stages based on the external morphological features of *Crocodylus porosus* (Crocodylidae), and they were followed by Ferguson (1985) for *Alligator mississippiensis* (Alligatoridae), *Caiman latirostris* (Alligatoridae) by Iungman et al., 2008. For the lepidosaurs, the morphological descriptions of embryonic stages have been well represented in studies conducted for the families Lacertia and Chamaleonidae (Arias and Lobo 2006; Dufaure and Hubert 1961; Rieppel 1993). For the iguanids, the more relevant work belongs to the representatives of the family Tropiduridae in the *Liolaemus* genus (Abdala et al., 1996; Lemus, 1967; Lemus and Duvauchelle 1966; Lemus et al., 1981; Lobo et al., 1995, and). Álvarez et al. (2005) carried out a study on the embryonic stages of *Policrus acutrirostris* describing the chronology of the development of the bones and cartilages. Usually, most of these works describe some embryonic features; however, those who establish a complete series of ontogenetic development are very few. The most studies corresponding to species with embryonary retention, the early stages correspond to the intrauterine state. To compare the embryology of several vertebrates, it is required to describe the early development features. Although many species these data are not available, developmental staging tables for lizards include Lacertilia (Dufaure and Hubert 1961), Tropiduridae (Py-Daniel et al., 2017), Iguanidae (Iungman et al., 2019) and oviparous species (Blanc, 1974; Lemus et al., 1981; Muthukkaruppan et al., 1970; Sanger et al., 2008).

The calcareous cover of the eggs in Squamata is composed of an outer layer of inorganic character (shell) constituted by several layers of fibers (Fernández et al., 2013). The number of fiber layers varies between species and can be traversed by pores, as well as presenting variations at the morphological level of calcareous deposits (Packard and Packard, 1989; Wink et al., 1990). Some authors mention that the structure of the eggshell, at the time of oviductal transit and during incubation, undergoes changes both at the level of thickness and in the size of the pores (Simoncini et al., 2014). To understand the different physiological processes that occur during incubation and embryonic development, it is necessary to know these structural changes in the eggshell of reptiles (Simoncini et al., 2014). Within the oviparous reptiles, the structure of the shells in the Squamata is variable, which raises the possibility of a similar variability in the structure of the oviduct and the mechanism of shell formation (Pike et al., 2012).

The genus *Salvator* is represented by lizards belonging to the family Iguanidae. These lizards are large in size, oviparous, and distributed in South America (Ávila Pires, 1995; Harvey et al., 2012). Their oviposition activity is concentrated in the spring months, with the female placing up to 42 eggs (Fitzgerald et al., 1994; Yanosky and Mercolli 1991). These are white, soft to the touch, and of rough texture at the embryo side and smooth on the opposite side. The incubation period is approximately 72 days (Yanoski and Mercolli, 1995). Today this species has won interest in both ecological characteristics and economic exploitation. On the other hand, the natural population *S. merianae* (Duméril and Bibron, 1839) and *S. rufescens* (Günther 1871; formerly *Tupinambis merianae* and *Tupinambis rufescens*; Harvey et al., 2012), species represented in Argentina, are subject to intense exploitation (Fitzgerald et al., 1994) with authorized extraction quotas that have institutionalized their hunting.

Captive breeding of these lizards is an alternative for sustainable use, which also allowing their replacement in nature (Noriega et al., 1996; Sanger et al., 2008). One of the most complex phases of zootechnical management is nesting. In this process, a combination of physical and biotic factors contributes to providing the optimal conditions for embryonic development. However, details of its development had not been widely explored. Here we present a table containing the sequence complete of post-oviposition normal development and structure of the eggshell of *S. merianae* in the oviductal tract and during the post-oviposition embryonic development. This study provides the characteristics of its embryonic state based on the principal morphological transformations that the embryo could experience during the process of artificial incubation versus natural incubation.

2 | MATERIALS AND METHODS

2.1 | Eggs maintenance and embryos collections

This study was conducted with gravid females of *S. merianae* specimens raised in captivity in the province of Tucuman, Northern Argentina (26°51′S, 65°17′W). The studies were carried out with individuals of *Salvator*

merianae adapted to captivity. This study took reasonable precautions to prevent the animals from suffering stress or pain, according to the protocol of the institutional committee for the care and use of experimental animals (IACUC). After the period of copulations, females with signs of pregnancy were separated from the breeding stock and moved to individual nesting pens (Manes et al., 2007) with control of the physical conditions to estimate the moment of the egg-laying.

To have a correct sequence of the stages of development, the study was based on two egg-laying, selected according to the uniformity of size, color, and firmness of the eggs. To complete the initial states and chronologically adjust the description, two additional egg-laying was used, in which it was possible to determine precisely the beginning of the ovipositing (Oct–Nov/2012 and Oct–Nov2013).

The eggs were incubated in plastic boxes containing medium grain vermiculite, hydrated with a 2% copper sulfate solution to prevent microbial contamination (Manes et al., 2003). The incubation was carried out at a temperature of 29° ±0.5°C. The initial hydration of the substrate corresponded to a vermiculite water relationship of 1:1.4 (p/p), equivalent to a water potential of –50 kPa, calculated by the equation: $\Psi = 16.15e^{-0.025\ (\theta)}$, where Ψ is the water potential and θ the content of water (Tracy et al., 1978).

The fixation of the eggs was performed at intervals of 12 hr during the first 2 weeks, at intervals of 24 hr the following 4 weeks and intervals of 48 hr the remaining 4 weeks. In the end, 120 embryos were analyzed (the same was used for further studies, including ultrastructural eggshell, three embryos per stage), the employed fixative was the fluid of Duboscq-Brasil (picric acid 0.4%; ethanol 53%; formaldehyde 10.6%, acetic acid 0.7%). The embryos were euthanized by an overdose of Carticaine-L-adrenaline following recommendations by The Herpetological Animal Care and Use Committee (American Society of Ichthyologists and Herpetologists; Beaupre et al., 2004). After that, each embryo was measured and averaged for each stage of development.

2.2 | Development stage determination

The characterization of each stage was done based on the external morphological characters (branchial arches, eyelids, limbs, claws, pigmentation of the body, development of scales, and egg teeth). The embryos were carefully analyzed and compared with other lizards (*Lacerta vivipara jacquin* [Dufaure and Hubert 1961]; *Lioluemus gravenhorsti* (Lemus, 1967); *Lioluemus tenuis tenuis* [Lemus and Duvauchelle 1966, and Lemus et al., 1981]; *Gallus agllus domesticus* [Hamburger and Hamilton 1992]; *Polychrus acutirostris* [Álvarez et al., 2005]; *Caiman latirostris* [Iungman et al., 2008]; *Paroedura pictus* [Noro et al., 2009]; genus *Anolis* [Sanger et al., 2008]; *Eublepharis macularius* [Wise et al., 2009]; *Taeniopygia guttata* [Murray et al., 2013]; *Rhea americana* [Melo de Almeida et al., 2015]; *Salvator merianae* [Iungman et al., 2019]) also we considered other features that were not regarded by these authors.

The embryonic development was divided into early stages (Stage 1–24), middle stages (stage 25–32), and late-stages (Stage 33–40). For stages 1 and 2, the length of the zona pellucida, the length of the primitive streak, and the total length of the embryo were measured, considered from the anterior end of the neural plate/tube to the later end of the primitive streak.

2.3 | Obtaining the shells: Oviductal transit

For the case of obtaining the oviduct and oviductal eggs, by ultrasound (Garcia Valdez et al., 2011) a gravid female of *S. merianae* was detected, which was later sacrificed for analysis, following the standard method established in the Guide for Animal Euthanasia proposed by the IACUC (The Institutional Committee Animal Care and Use Committee 2013). For the study, the necessary precautions were taken to avoid stress and pain, according to the protocol of the Institutional Committee for the Care and Use of Experimental Animals (CICUAL) CICUAL 0004-2017 FM-UNNE.

The specimen was dissected, isolating the oviduct with eggs in transit, proceeding to take a tissue fragment of shell eggs the three regions: infundibulum, tubal portion, and uterus, which were fixed with Duboscq-Brasil and then preserved in 70% alcohol. These sections were processed following the conventional protocol for Scanning Electron Microscopy (SEM), which consisted of dehydration in solutions of increasing concentration of Acetone (12.5, 25, 50, 75, and 100%), drying at a critical point, and gold plating. The observations were made in a JEOL JSM-5800 LV.

2.4 | Obtaining the shells: Post-posture

In this study, dorsal, ventral and lateral sections of a total of 78 shells were analyzed, of which 11 corresponded to eggs in oviductal transit and 67 to eggs spawned from females adapted to captivity, from the hatchery of the Faculty of Zootechnics of the University National de Tucumán, were moved to individual nesting sites (Manes

et al., 2007). The unrotated eggs were immediately included in trays containing medium grain vermiculite, hydrated with 2% copper sulfate solution to prevent microbial contamination (Manes et al., 2003). The incubation was carried out at a temperature of 29.5°C. The fixation of the eggs in toto was carried out at 12 hr intervals during the first 2 weeks, at 24 hr intervals the next four and 48 hr intervals the remaining four. The Duboscq-Brasil fluid was used as a fixative and then preserved in 70% alcohol.

Following the proposal by Simoncini et al. (2014) for *Caiman latirostris*, the total incubation days were divided into thirds: first third (1–24 days of incubation), second third (25–52 days of incubation), and third (to 53–73 days of incubation). The total samples were subjected to the conventional MEB protocol as well as the oviduct.

3 | RESULTS

3.1 | Ultrastructure of the eggshell of *S. merianae*

3.1.1 | Oviductal transit

The analyzed oviduct presented a total of 13 eggs, the first three eggs next to the infundibulum, did not show an oviductal cover. The remaining eggs exhibited a sequence in the arrangement of fibers and amorphous material on the eggshell (Figure 1). Initially, the fibers appear cohesive due to the presence of amorphous material, evidencing the initial deposition of a new fibrous layer (Figure 1a,b). In the oviductal transit to the uterine region, the fascicular organization of the newly formed fibers is visualized (Figure 1c,d). The internal fibers are joined by amorphous material. By observing changes in orientation of the superficial and deep fibers, the arrangement on the surface is described as reticular. In contrast, in the deep fibers, the further deposition of the amorphous material is observed (Figure 1d,e). In the region near the cloaca, the shell structure of the eggs in transit is bilaminar, differentiating an internal and an external membrane (Figure 1f).

3.1.2 | Incubation period

During embryonic development, a close relationship is established between the embryo and the shell (Figure 2). There is evidence of a change in location from the early stage in which the embryo is immersed in the yolk mass (Figure 2a) until it is separated once the extraembryonic membranes are established. The vascularization begins to increase (Figure 2a–c). The increase in the diameter of the chorion and allantois membranes (Figure 2d) can be seen during the middle stage of development. Finally, in the late stage, the embryo occupies most of the egg, and the extraembryonic membranes are entirely attached to the shell of the egg, covering 90% of its surface (Figure 2e).

3.1.3 | Micro-structural characteristics of the shell

The shell structure of *S. merianae* egg during embryonic development exhibits three layers: an outer crust of plates with calcium carbonate crystals in the form of calcite (Figure 3a). Below we found a thick layer of strongly compacted fibers and a thin amorphous inner limiting layer (Figure 3e,g,h,j).

In the outer crust of a recently spawned egg (first third) fibers and amorphous material are observed (Figure 3a,d), as embryonic development progresses, during the second third, limestone plaques limited by furrows and rosetta crystallizations are observed (Figure 3e,h). In the region where the embryo is located in the egg externally, a concentration of rosettes could be observed, which increases in number and compaction during the third, in these stages a thinning of the skin can also be observed (Figure 3i,h).

The fibrous middle layer at the time of egg-laying (first third) appears as a thick layer of loose fibers (Figure 3a). As the embryonic development progresses (second third), the fibrous layer becomes markedly compact (Figure 3g,h). Finally, in the last third, the distinction between this layer and the inner one becomes imperceptible (Figure 3j).

The internal membrane when egg spawning occurs (first third) is composed of fibers and amorphous material, as seen in oviductal eggs close to spawning (Figure 1f), as the ontogenetic development progresses (second third). Greater compaction is visualized, and it comes into contact in some regions with the chorion membrane and the allantois (Figure 3f,h). Towards the end of embryonic development (third), greater compaction is evidenced, and the individualization of the fibrous membrane becomes imperceptible. The large vessels of the extraembryonic membranes cover the largest surface of the egg (Figure 3j,k).

3.1.4 | Developmental embryonic of S. merianae

Here, we describe the post-oviposition embryonic development of *S. merianae*. We based on morphological features.

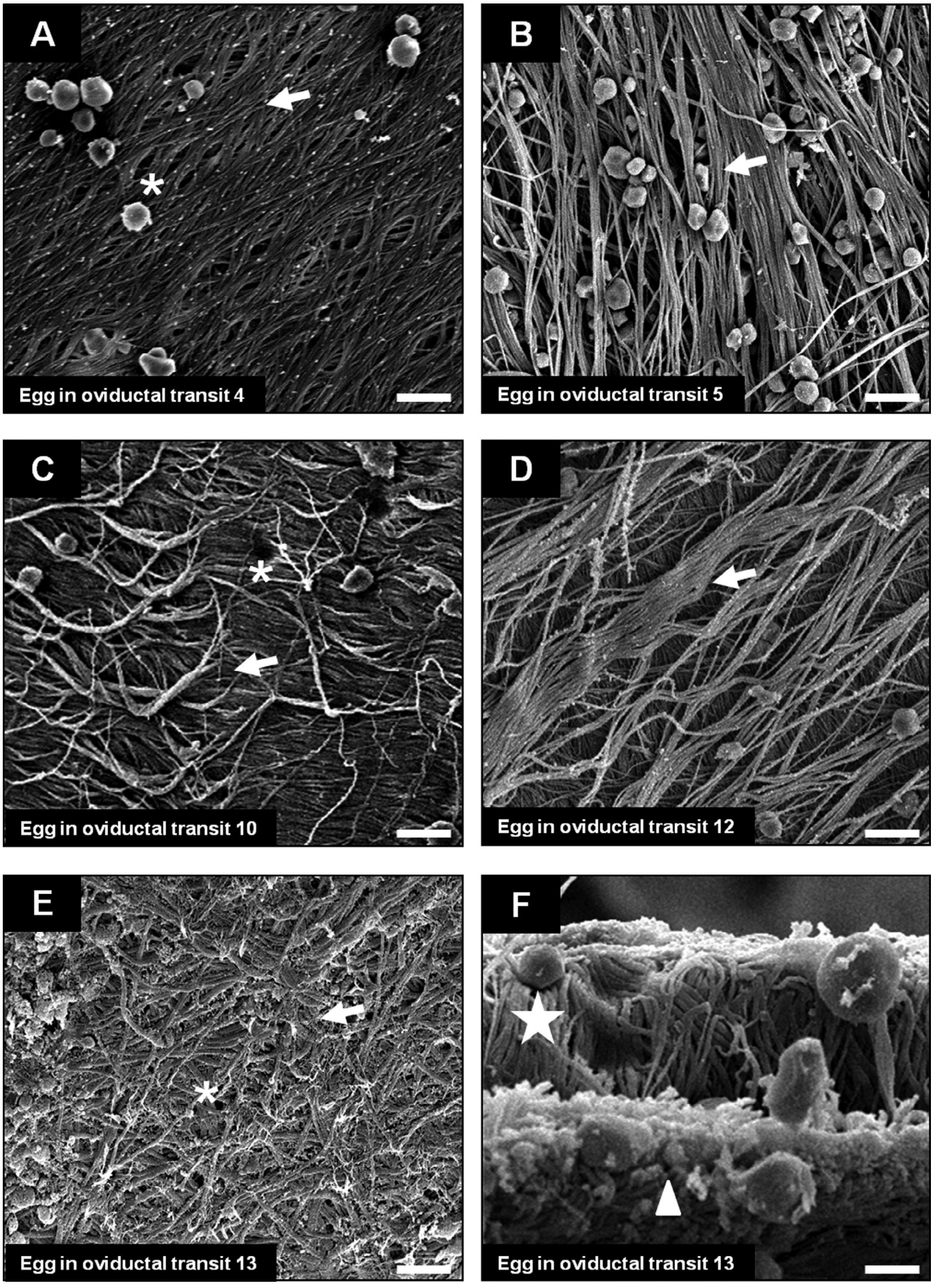

FIGURE 1 Legend on next page.

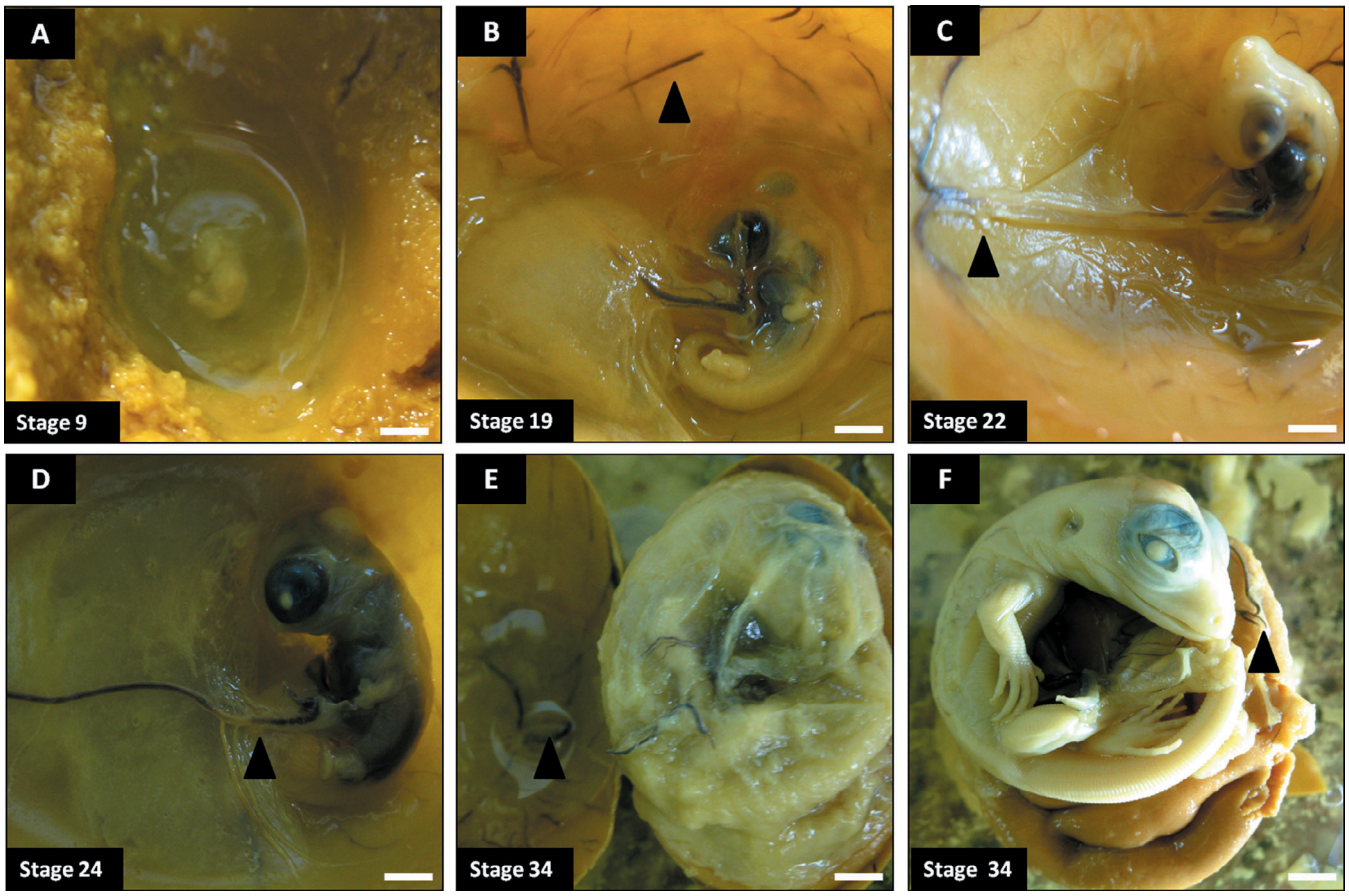

FIGURE 2 Relationship between the embryo of *S. merianae*, its location, and vascularization concerning the shell during embryonic development. (a–c) Embryos corresponding to the early stage of development. (d) Embryo corresponding to the middle stage of development. (e and f) Embryo corresponding to the late stage of development. References: arrowhead: vascularization. Scale: (a–c) 2 mm and (d–f) 5 mm

3.1.5 | Early stage (stages 1–24)

The early stage of embryonic of *S. merianae* was comprised of 24 stages (Figure 1), from the start of incubation corresponding to the primitive streak, curly body of the C-shape embryo until that the maxillary and the mandibular process have been fused with the frontal process and the forelimb with the plate digital. (Figures 4 and 5).

Incubation start

At the time of oviposition, embryos presented initial development characters such as gastrulation. Two areas are visible in a clear area, which corresponds to the zona pellucida (pa) and the opaque area (a) with an inverted pear-shape. Primitive streak (ps) is visible in the rear end of the zona pellucida (Figure 4a).

Stage 2 (embryo 12 hr) *Somites* (s): 10 pairs are present on both sides of the spinal cord. The notochord passes the neural tube. Unfused neural folds (nf) primitive pit. Full length: (ps + length the nf) 2.34 mm. Tubular heart. Yolk sac membrane with blood islands, vitelline vein flow emerges from the region of the heart, while the vitelline artery is found along the sidewalls of the body. The amnios (am) covers the embryos from previous regions. We observed a condensation in the anterior mesoderm regions similar to allantois (al) (Figure 4b).

FIGURE 1 SEM micrograph of the eggshell of *S. merianae* during oviductal transit. (a) Detail of the fourth egg in transit in dorsal view. (b) detail of the arrangement of the fiber in the fifth egg in transit (dorsal view). (c) detail of the arrangement of the fiber in the tenth egg in transit (dorsal view). (d) The detail in the dorsal view of the oviductal transit egg before to the laying. (e) Transverse view of the eggshell showing the two membranes (internal and external). References: asterisk: pores. Arrow: fibers. Star: outer membrane. Arrowhead: inner membrane. Scale: 600 μ

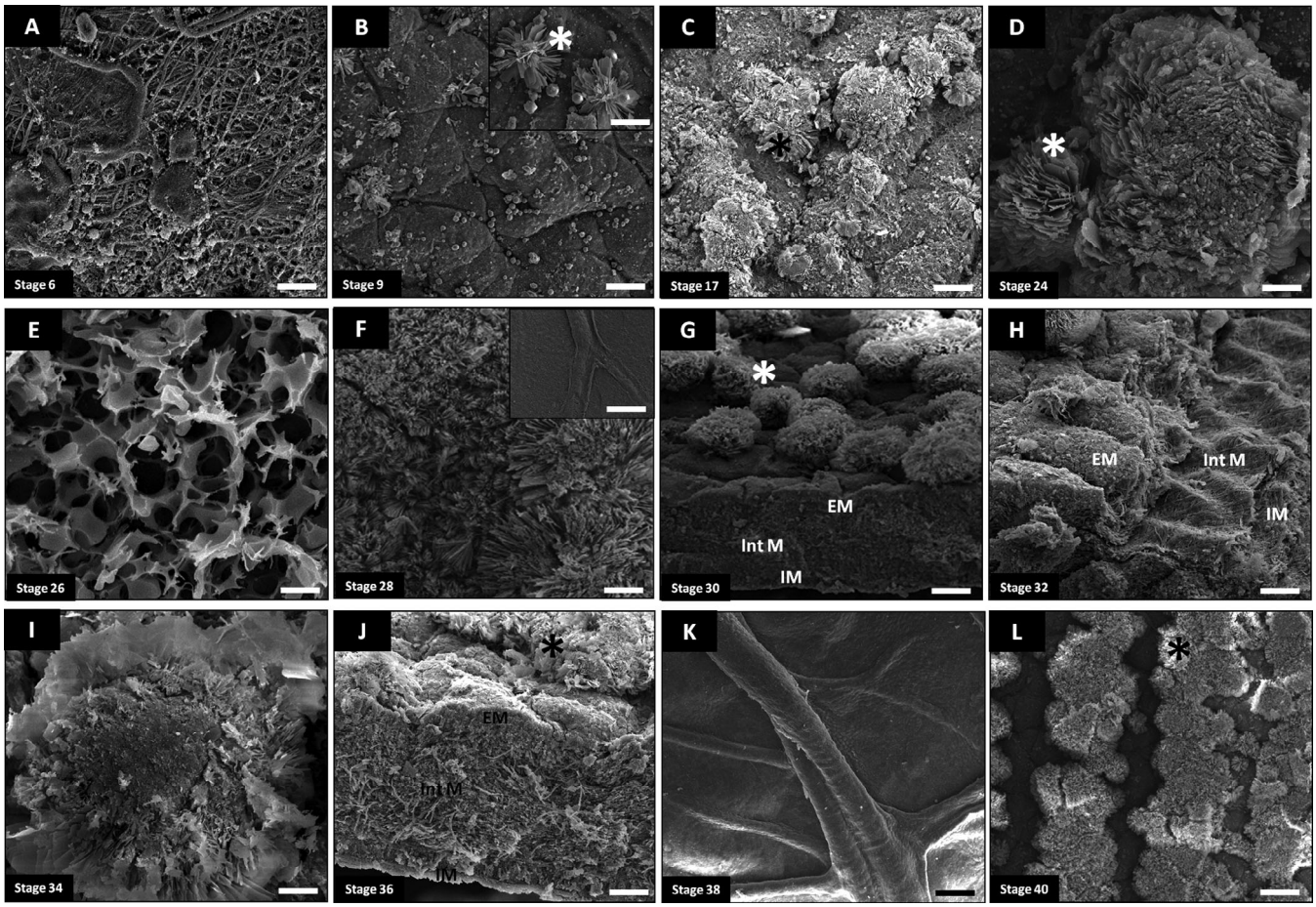

FIGURE 3 SEM micrograph of eggshells of *S. merianae* posture. (a–d) detail of the shell during the early stage of embryonic development; (a–c) dorsal region; (d) detail of the calcareous rosettes. (e–h) detail of the shell during the middle stage of embryonic development; (e) detail of the internal membrane. (f) Dorsal region of the shell with vascularization detail. (g) cross-section of the shell, the outer or calcareous membrane, the fibrous membrane, and the internal membrane are evident. (h) detail of the three membranes that make up the shell of the egg. (i–k) detail of the shell during the late stage of embryonic development; (i) detail of a calcareous rosette. (j) cross-section of the shell where the compaction of the three membranes is evident. (k) vascularization of the allantois membrane. (h) detail of the calcareous rosettes on the dorsal side of the egg. References: asterisk, calcareous rosettes; EM, outer membrane; IntM, fibrous intermediate membrane; IM, internal membrane. Scale: a, b, c, f, g, h, j, l: 600 μ. d, e, i, k: 1,000 μ

Stage 3 (embryo 24 hr) *Somites* (s): 12 pairs. The body has completely rotated to the right. Full length (FL): (ps + length the nf) 3.69 mm five brain vesicles are visible: regionalization of forebrain into telencephalon, diencephalon, midbrain, hindbrain, and myelencephalon. The curvature of the wing head height hindbrain. The first branchial arch (ba) is distinct. Heart (h) slightly twisted. The crystalline is turned inside, and the optic cup is observed. The otic placode is visible at the height of the rhombomeres four and five. The allantois is an outline of the saccular aspect that appears as a small ventral swelling (Figure 4c).

Stage 4 (embryo 36 hr) *Somites*: 17 pairs. Embryos have a j-shaped inverted. *FL*: 3.9 mm. Heart whit S-shaped laterally expanded to the right. Optic cup and crystalline larger, the otic placode are invaginated. The optic vesicle (ov) has a horseshoe-shaped, without pigmentation. First and second (hyoid arch) arches are distinct. The tubular heart (h) presents torsion. The allantois is outlined next to the ventral caudal region larger than the previous stage. The vitelline membrane has major vessels (Figure 4d).

Stage 5 (embryos 72 hr) *Somites*: 23 pairs, initiation of caudal flexure FL: 4 mm, well-developed midbrain. The skin was thin and allowed visualization of the heart, shows an S-shaped form, and it is displaced to the left, cardiac septa are distinct. Atrial and ventricular chambers differentiated. Three branchial arches project over the surface. The first and second visceral grooves are cleft, but they are only present on the dorsal third of the first groove and the dorsal half of the second one. The otic vesicle invaginates, and the nasal placode is evident. The allantois is growing (Figure 4e).

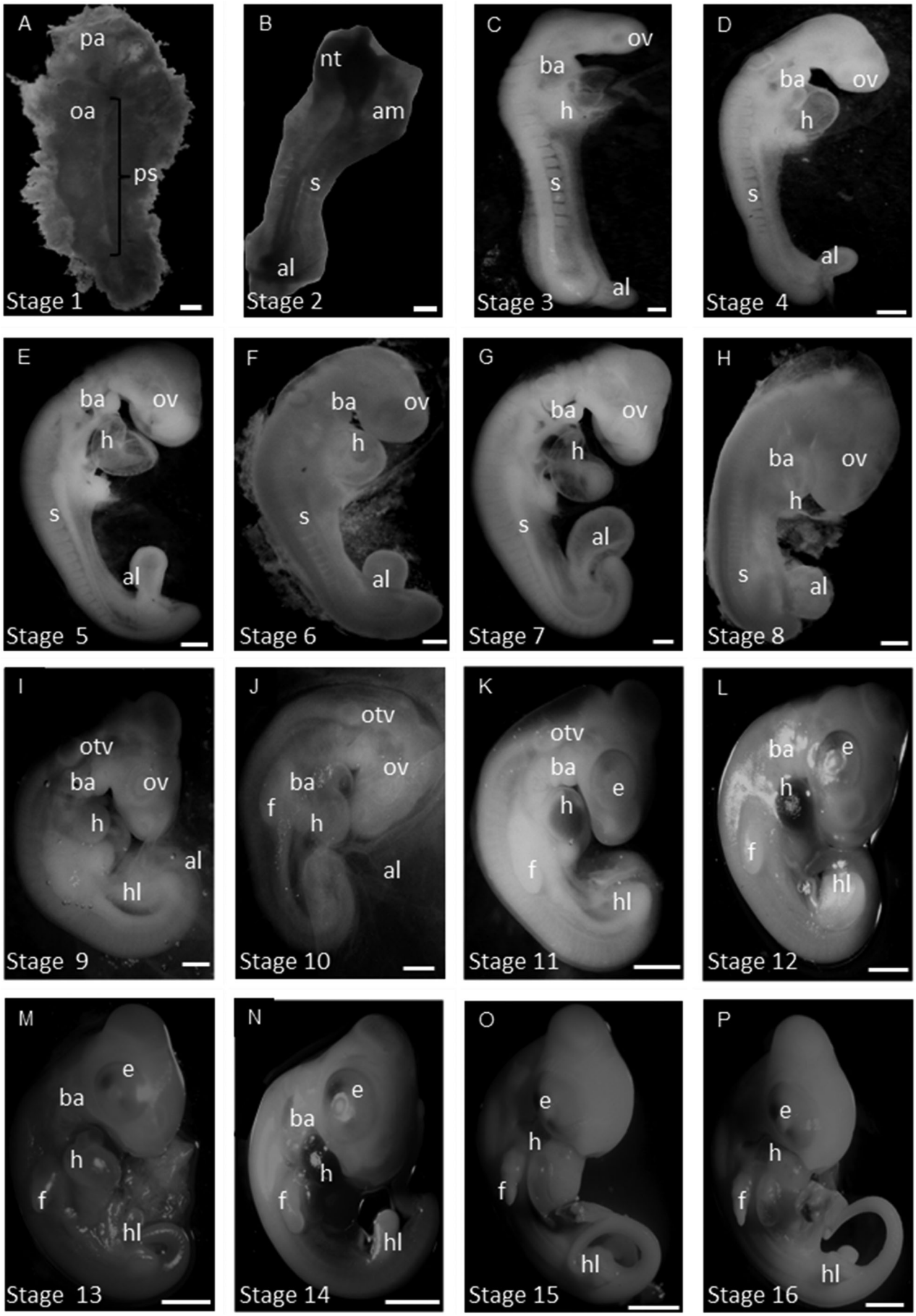

FIGURE 4 Legend on next page.

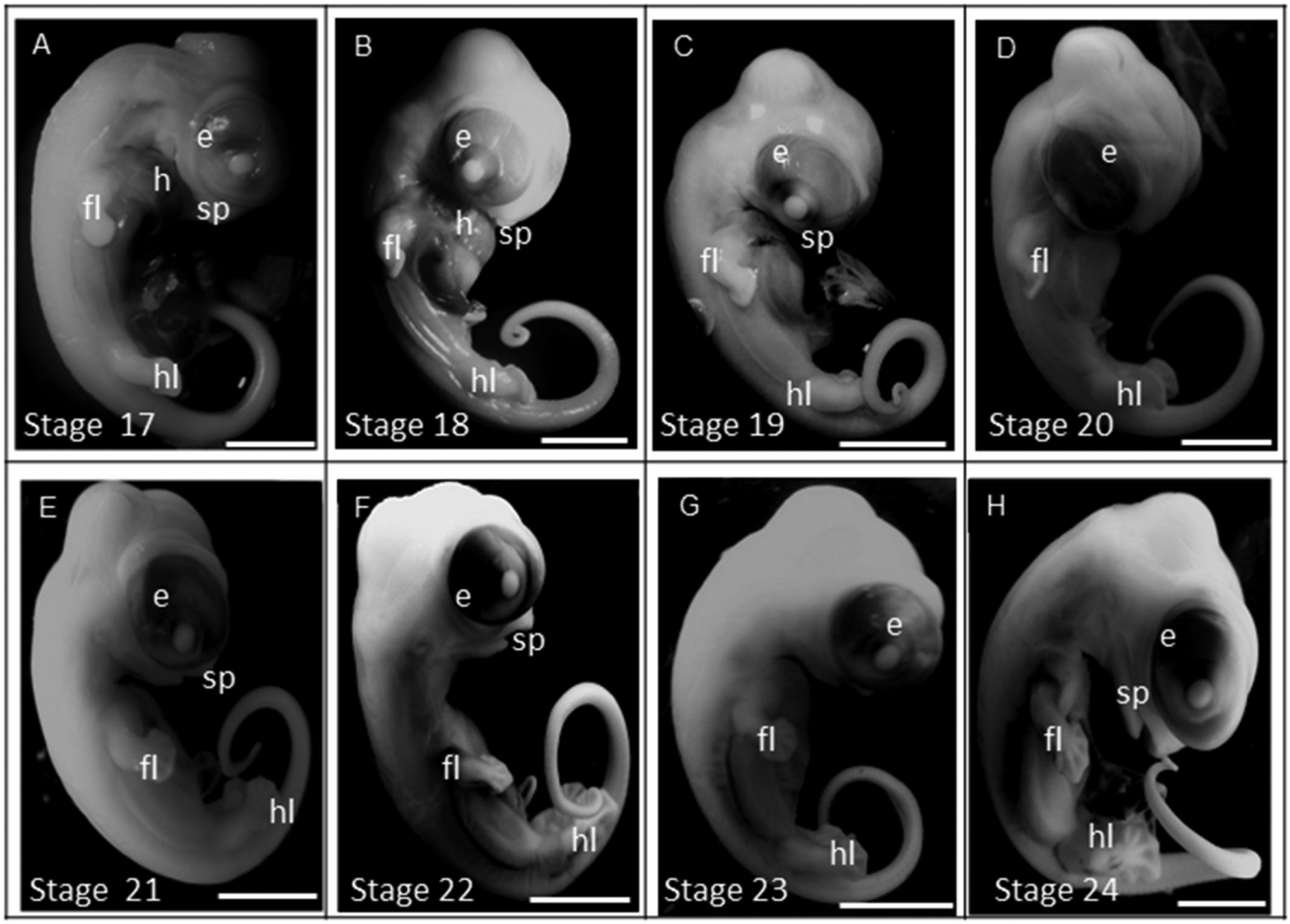

FIGURE 5 Post-ovipositional development of *S. merianae* at early phases of development (stages 17–24). Scale Bars = 5 mm. Lateral view. (a) Stage 17, (b) Stage 18, (c) Stage 19, (d) Stage 20, (e) Stage 21, (f)Stage 22, (g) Stage 23, (h) Stage 24. e, eyes; fl, forelimb; h, heart; hl, hindlimb; sp, splanchnocranium

Stage 6 (embryo 3½ days) *Somites*: 26 pairs. The embryo maintains the shape of an inverted J. Body torsion has commenced. Caudal flexure is more pronounced. FL: 4.02 mm. There are three branchial arches, and the heart is more flexure. The crystalline and choroid pits were evident, the amnion is completely closed, and the allantois is more prominent in size (Figure 1f).

Stage 7 (embryo 4 days) *somites*: 28 pairs. FL: 4.4 mm. The rhombomeres are seen. Three branchial arches are distinct. The otic vesicle is completely invaginated without endolymphatic duct; optic cups completely invaginate with crystalline totally incorporated. An inconspicuous condensation of mesoderm is present at the forelimb-level. The liver is an asymmetric bulge lying under the heart. The allantois is longer than the previous stages (Figure 4g).

Stage 8 (embryo 4½ days) *Somites*: 33/34 pairs. *Body*: FL: 5.02 mm. Flexure of the embryos is more pronounced, (*Tail*) flexures ventrally. The telencephalon was divided into two vesicles seen laterally; the epiphysis, in the dorsal region of the diencephalon, is not visible. The mesencephalon divided into two prominent lobes. Complete torsion of the heart, there are still distinct tree branchial arches. The optic vesicle is pigmented for the first time; is the visible first indication of nasal placode pits. The allantois is swollen, reaching the length of the *Tail*.

FIGURE 4 Post-ovipositional development of *S. merianae* at early phases of development (stages 1–16). Scale Bars = stage (1–3) 2 mm. stage (4–10) 2 mm stage (11–16) 5 mm. (a) Stage 1: pa: Area pellucid; oa: opaque area; ps: primitive groov. (b) Stage 2: nt: neural tube; am: amnios; s: somites; (c) Stage 3, (d) Stage 4, (e) Stage 5, (f) Stage 6, (g) Stage 7, (h) Stage 8, (i) Stage 9, (j) Stage 10, (k) Stage 11, (l) Stage 12, (m) Stage 13, (n) Stage 14, (o) Stage 15, (p) Stage 16. al, allantois; ba, Branchial arch; e, eyes; f, forelimb; h, heart; hl, hindlimb; otv, otic vesicle; ov, optic vesicle

The vitelline membrane has vessels and arteries, and the hindlimb appears at the level to somite 13 and 16 (Figure 4h).

Stage 9 (embryo 5 days) The somites do not make distinguishable. The flexure of the body begins with the trunk at the thoracic level; the heart is visible. FL. 5.6 mm. The mesencephalon is prominent, and mesencephalon vesicles are visible. Four branchial arches are visible. Complete torsion of the heart, with more defined compartmentalization. The optic vesicle is developing without pigmentation of the retina; the otic vesicle is present. The allantois is bigger than in the previous stage. The primordial limb areas remain flat. The mesoderm is condensed in the area of the forelimb and hindlimb (hl) but is not clearly defined. *Tail* curled (Figure 4i).

Stage 10 (embryo 7 days) FL: 6.3 mm. Four branchial arches are well differentiated. The heart is the same previous stage. In the otic vesicle, we observed the choroid fissure and the retina differentiated, but unpigmented. The nasal placode with pits appears; the otic vesicles are connected to the small ectoderm opening by the endolymphatic duct. The forelimb is bigger than in the previous stage, but the hindlimb is absent. The allantois is the same size as the embryo, and blood vessels appear-outline of liver and kidney are seen by transparency (Figure 4j).

Stage 11 (embryo 8 days) FL: 6.8 mm, Four branchial arches, the first arch presents the maxillary and mandibular processes; the four is of smaller size. Eyes (e) have a darkly pigmented retina. The otic vesicle is connected by a small opening in the ectoderm, endolymphatic duct, and nasal slits more pronounced. The heart begins to be incorporated within the body. The allantois is bigger. The yolk sac has a great vascularization. The forelimb buds have grown ventrally with a caudal slant. The mesoderm is condensed in the area of the hindlimb. *Tail* curled. (Figure 4k).

Stage 12 (embryo 9 days) FL: 7.1 mm. The mesencephalon is bigger than in the previous stage; four branchial arches are visible (the forth is present but inconspicuous) mandibular and maxillary processes are developed. Nasal pits more pronounced. The heart is incorporated into the body. The eye is stronger pigmented; choroid fissure still lacks pigments. The allantois is bigger. Vitelline veins emerge from the caudal limit of heart. In contrast, the vitelline arteries run along the lateral walls of the body, sticking out at approximately the caudal third of the embryo. The Limbs are lengthened and have thickened significantly to appear knob-like in shape. The forelimb bud is thicker than the hindlimb bud, although both are still equal in length. Digit formed in forelimb and hindlimb. *Tail* curled. (Figure 4l).

Stage 13 (embryo 10 days) FL: 7.8 mm, the rostral border of the mandibular process is located at the caudal edge of the lens. The fourth branchial arch is a little visible. The eyes have a darker pigmentation on the retina. The interior chambers of the heart have become increasingly obscured due to the thickening of the pericardial epithelium. The forelimbs buds are further elongated so that the hindlimbs extend past the *Tail*. The elbow joint has become more acute than in the previous stage. The elbow flexure is distinct. Constriction of the wrist and ankle are accentuated from the previous stage (Figure 4m).

Stage 14 (embryo 11 days) FL: 10.37 mm. The first ventricle of telencephalon has increased in size to exceed the diameter of the eye. The fourth branchial arches are not visible. The maxillary process is longer than the mandibular process. Increased retinal pigmentation is present in the upper regions of the eye, the diameter of the eye (diameter: 2.2 mm). The heart is incorporated into the body. The limb buds are elongated so that the forelimb buds have obscured the dorsal region of the ventricle, and the hindlimb (hl) buds have obscured part of the *Tail* bud. Curly *Tail*. (Forelimb Length (LF): 0.85 mm, width forelimb (FW): 0.45 mm; length hindlimb (HL): 0.10 mm, width hindlimb (WH): 0.4 mm; Figure 4n).

Stage 15 (embryo 12 days) LT: 10.85 mm. The hindbrain is smaller (it has become shorter and thinner) about the head, and its walls are thicker now. The branchial arches are not visible. The first visceral cleft is sinusoidal in the outline, situated above the otocyst. The maxillary processes fused dorsally to the frontonasal process, forming a continuing base beneath the eyes and the medial and lateral nasal processes. The lower jaw extends beneath maxillary processes up to the middle of the eyes. The eyes have protruding eyeballs. The nictitating membrane has developed in the anterior corner of the eyes. The thoracic walls begin to cover the heart. The main segments of the forelimbs and hindlimbs are demarked. The limbs are slightly flexed at the elbow-joint and knee-joint level. The digital plate is present, but still smooth. The bud genitalia is visible from the ventral side of the hindlimbs buds. The *Tail* is still curled (Figure 4o).

Stage 16 (embryo 13 days). LF: 14.13 mm. The embryo presented a whitish color. The organs in the body are not very visible. The hindbrain is not visible, while midbrain forms a prominent bulge. The olfactory bulbs are clearly distinct. The stomodeum plate is unperforated. The thoracic wall is covering the heart. The eyes were big with a diameter larger (2.98 mm) also homogenous pigmentation. The allantois size remains in previous stages (diameter: 2.4 mm). The limbs are more elongated; forelimbs are slightly longer than hindlimbs. The *Tail* is still

curled. (LF: 2. 98 mm WF: 1.78 mm, LH: 0. 4 mm and WH: 0. 56 mm; Figure 4p).

Stage 17 (embryo 14½ days) LF: 15.36 mm. The lengthening of the neck and jaws continues. The splanchnocranium and the maxillary process fused to the frontonasal process, which will become the external nares. The eyeballs and jaws are developing, and they constitute most of the skull space. (Diameter: 2.01 mm). The forelimbs start the demarcation of five fingers (LF: 2 mm; LH: 1. 92 mm) but not in the hindlimb (Figure 5a).

Stage 18 (embryo 15 days) FL: 16.32 mm. Brain lobes are still visible, but the top of the skull has almost closed posteriorly. The splanchnocranium maxillary and mandibular processes are fused to the frontal process. The first plate and second arch are fused in the middle line. Stomodeum is now perforated. The nasal processes coalesced at the middle line displacing nostrils dorsally. The auditory cleft is differentiated. The heart is fully incorporated into the body. The eyes have pigmented retina (eyes diameter: 4.08 mm and crystalline diameter 1.2 mm). The forelimb with a digital plate (LF: 2.3 mm and WF: 1 mm). The hindlimb with two digital plates (LH: 2.1 mm and WH: 1 mm). External genitalia primordium reaches the height of cloaca lips (Figure 5b).

Stage 19 (embryo 17 days) FL: 16.58 mm. In the splacnocranium, the snout begins to form. The heart is large. The eyelids outline an oval circumference reaching the eye's white ring (diameter: 4.71 mm). Limbs, paddle-shaped is more evident in forelimbs than hindlimbs. The interphalangeal furrows have deepened, but digits have not yet separated. The articulation between the autopodium and zeugopodium, digital plate 1, and 2 between 2, 3, and 3, 4 digits are visible. (LF: 2.98 mm and WF: 1.88 mm; LH: 2.82 mm and WH: 1.88 mm; Figure 5c).

Stage 20 (embryo 20 days) FL: 17.72 mm. The maxillary process is now located immediately caudal to the frontal process; the tongue is visible. In the eyes increased retinal pigmentation (diameter 5.96 mm.); the eyelids overlay 25% of the eyes. The forelimbs and hindlimbs allow the further individualization and flattening of the autopodium, forming the digital plate (LF: 5.49 mm; LH: 4.71 mm; Figure 5d).

Stage 21 (embryo 21 days) *Body*: FL: 18.30 mm. The auditory meatus is merely a cleft laying immediately after the dorsal limit of the eye. The external naris stills a narrow slit. The eyes are larger. The forelimbs and hindlimbs have a phalanx. A series of bulges in the digits mark the beginning of the interdigital joints (Figure 5e).

Stage 22 (embryo 22 days) FL: 18.63 mm. The splacnocranium, mandibular, and maxillary processes continued to migrate in a rostral direction to meet the frontal process. The conjunctival papillae are not distinguishable. The forelimbs and hindlimbs are larger in size. The fore and hind limb autopodium with recesses between all digits (Figure 5f).

Stage 23 (embryo 23 days) *Body*: FL 18.97 mm. The mandibular and maxillary processes form a distinguishable snout. In The forelimbs and hindlimbs, the interphalangeal furrows deepened, but digits have not yet separated. The condensations of the middle digits are faintly visible in both limbs (Figure 5g).

Stage 24 (embryo 24 days) FL: 19.28 mm. The maxillary and mandibular processes are longer and curved downwards. The neck is differentiated. The lower eyelid overlaps the iris ventrally. The forelimbs and hindlimbs have a well-defined digit. The interdigital membranes are translucent. (Figure 5h).

3.1.6 | Middle stages (stage 25–32)

In the middle stage of embryonic development of *S. merianae* eight stages are recognized, the scales begin to delimit, the eyelid appears, and also the claws of toes and fingers cornification and initiation of pigmentation appear (Figure 6).

Stage 25 (embryo 25 days) FL: 19.62 mm. L. *Tail*: 20.6 mm. The snout is developing. The eyelid has advanced to cover the retina but only the outermost margins of the retina. The auditory capsule and auditory pit are marked. The digits are formed in forelimbs and hindlimbs interdigital membranes are reduced, more marked in forelimbs. Five digits are marked (LF: 5.49 mm; LH: 4.71 mm. The dorsal and caudal scales begin to delimit (Figure 6a).

Stage 26 (embryo 27 days) FL: 22.76 mm. *Tail*: 3.4 cm. The egg tooth appears. The snout is development. The eyes with pigmented retina are obscured (6.12 mm). The auditory capsule is the same previous stage. The forelimbs and hindlimbs have interdigital membranes that are fully retreated in all digits (LF: 6.75 mm; LH: 8.47 mm). The Dorsal and caudal scales have an imbricated position (Figure 6b).

Stage 27 (embryo 29 days) FL: 25.57 mm; *Tail*: 4.00 cm. The third ventricle of the diencephalon is not visible. The external nares are rounded. The auditory capsule is perforated. The eyelid covers 25% of the eye (6.12 mm). The forelimbs and hindlimbs have digits marked; nails are distinct on both fingers and toes. (LF: 9.73 mm; LH: 14.91 mm). Dorsal and caudal scales are the same as the previous stage, flakes appear ventral (Figure 6c).

Stage 28 (embryo 33–36 days) FL: 25.61 mm. *Tail*: 4.3 cm. The superior part of the skull is not posteriorly closed yet. The snout is more pronounced. The auditory

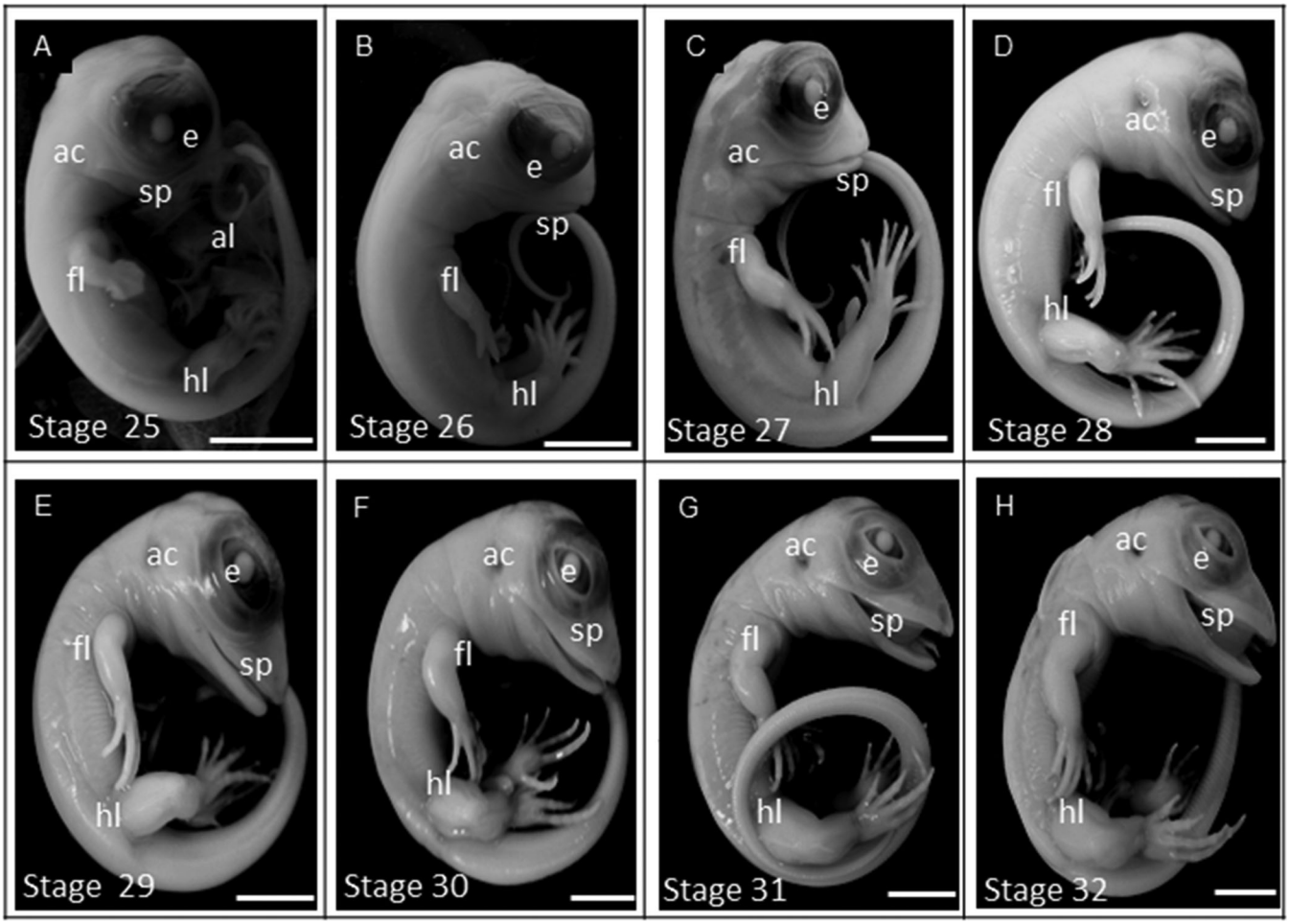

FIGURE 6 Post-ovipositional development of *S. merianae* at middle stages of development (stages 25–32). Scale Bars = 20 mm. Lateral view. (a) Stage 25, (b) Stage 26, (c) Stage 27, (d) Stage 28, (e) Stage 29, (f) Stage 30, (g) Stage 31, (h) Stage 32. al, allantois; ac, auditory capsule; e, eyes; fl, forelimb; hl, hindlimb; sp, splachnocranium

capsules are present laterally on the skull. The eyelid width is uniform; eyelid covers 35% of the eye (6.54 mm). The forelimbs and hindlimbs have tips slightly curved and enclosed in sheaths (LF: 11.42 mm; LH: 18.28 mm). The scales are present on all the body (Figure 6d).

Stage 29 (embryo 36–40 days) FL: 30.96 mm, *Tail*: 5.3 cm. The brain is at the same level as the skull in previous stages. The snout is more developed than in previous stages. The auditory capsules have a tympanum anlage. The eyelids cover 45% of the eyes, next to the lens (7.85 mm). The forelimbs and hindlimbs claws are flattened laterally and curved ventrally, the onset of cornification (LF: 13.86 mm; LH: 19.82 mm. The scales which are on flanks and neck are fusing at the ventral part of the jaws. There are sparse pigments along with the head (Figure 6e).

Stage 30 (embryo 40–44 days) FL: 32.34 mm, *Tail*: 5.8 cm. The snout is expanded. The oval eyelids have become more prominent, covering about half of the eyes. The auditory capsule is well-formed. The forelimbs and hindlimbs claws are fully formed (Figure 6f).

Stage 31 (embryo 44–48 days) FL: 33.57 mm. *Tail*: 7.7 cm. The snout is longer than the previous stages (MXP: 15.07 mm, MBP: 12.88 mm). The otic capsule is present. The eyelids are oval in shape (8 mm). The forelimbs and hindlimbs are more developed than in previous stages. The dorsal and caudal scales are pigmented (Figure 6g).

Stage 32 (embryo 48–52 days) FL: 35.04 mm. *Tail*: 8.2 cm. The snout is more developed than in previous stages. The cephalic plates begin to delimit. The otic capsule is more pronounced than in previous stages. The eyes are almost closed. The forelimbs are more developed, and hindlimbs have more developed shank. The scales have a scapular and ventral pigmentation (Figure 6h).

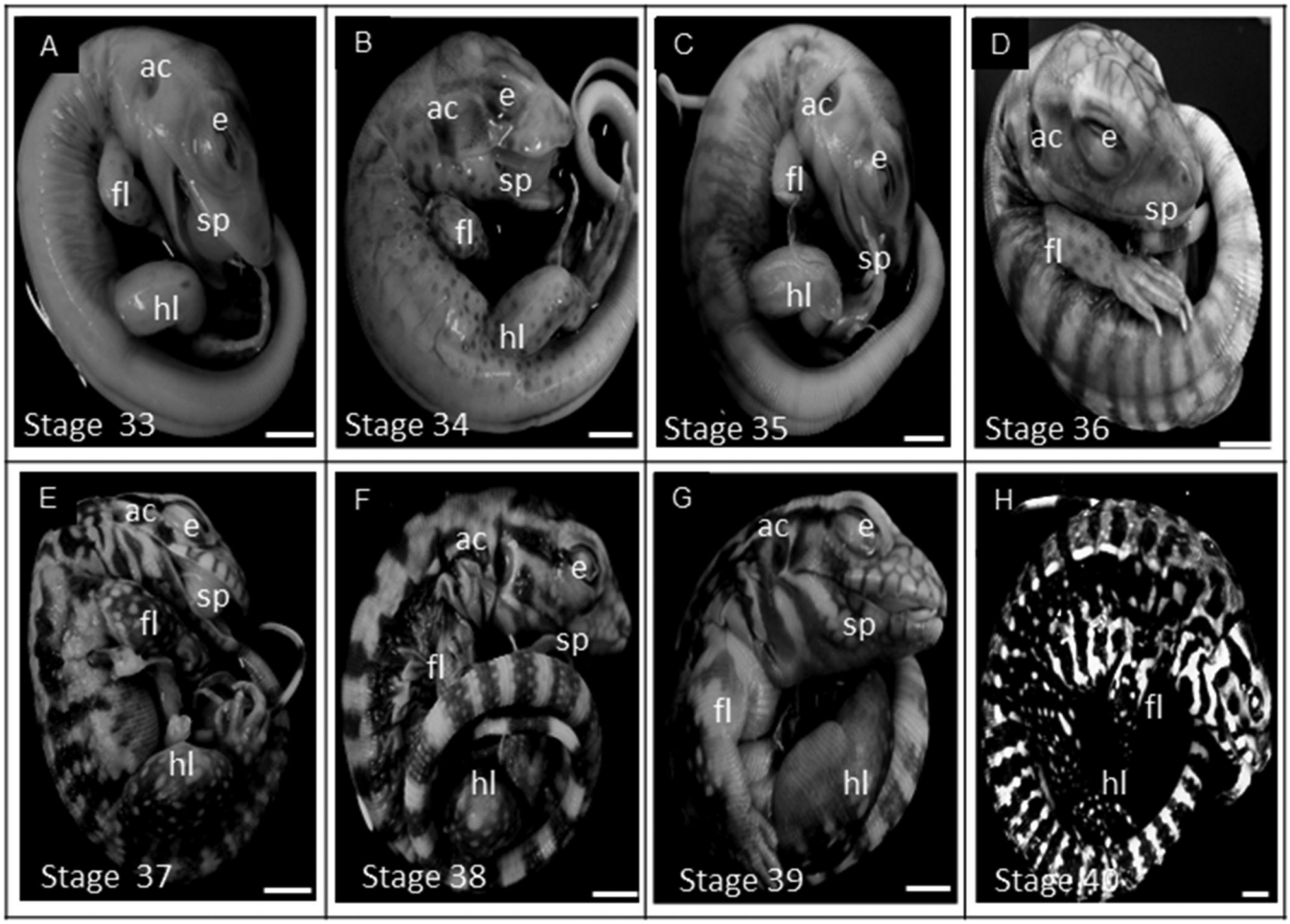

FIGURE 7 Post-ovipositional development of *S. merianae* at late stages of development (stages 33–40). Scale Bars = 2 cm. Lateral view. (a) Stage 33, (b) Stage 34, (c) Stage 35, (d) Stage 36, (e) Stage 37, (f) Stage 38, (g) Stage 39, (h) Stage 40. ac, auditory capsule; e, eyes; fl, forelimb; hl, hindlimb; sp, splachnocranium

3.1.7 | Late stages (stage 33–40)

In the late stages of embryonic development of *S. merianae* seven stages were identified, before hatching, this stage is characterized by the beginning of the delimitation of the scales, and also the cornification and initiation of the pigmentation of the claws of toes and fingers (Figure 7).

Stage 33 (embryo 52–55 days) FL: 35.08 mm. *Tail*: 9.2 cm. The preocular ridges appear, but become more prominent later in the development. The snout wall is robust; the eyelid upper lid tissue has scouts and is pigmented and covers the crystalline. The forelimbs and hindlimbs claws formation is complete, and the hooking becomes more marked toward hatching. A groove runs along the external surface of the claws are visible. The pigmentation has extended toward the body. The cephalic plate is differentiated (Figure 7a).

Stage 34 (embryo 55–57 days) FL: 35.41 mm. *Tail*: 10.4 cm. The maxillary and mandibular plates are delimitated; *maxillary process* length (LPM):12.68 mm and mandibular process length (LPM): 11.87 mm. The lower eyelid covers less than half of the pupil. The otic capsule is covering the neck crease. The forelimbs and hindlimbs are pigmented. The pigmentation has increased, giving the animal a light black color, but the dorsal aspect is still unpigmented or pale. The dorsal stripes are present (Figure 7b).

Stage 35 (embryo 57–59 days) FL: 35.62 mm. *Tail*: 11.1 cm. The maxillary process length (LPM): 15.51 mm and mandibular process length (LPM): 14.41 mm. The otic capsule is larger. The upper and lower eyelids are next to each other. The forelimbs and hindlimbs are robust. The scales are evident throughout the embryo surface; the pattern of adult dorsal own coloration is set (Figure 7c).

Stage 36 (embryo 59–61 days) FL: 35.75 mm. *Tail*: 12.6 cm. The snout is. Shorter. Maxillary process length (LPM): 13.64 mm and mandibular process length (LPM): 12.98 mm. A fold covers the otic capsule. The upper

eyelid and lower eyelid are in contact with each other. The forelimbs have pigmentation similar to juveniles. The pigmentation is stronger, so the embryo is brown now (Figure 7d).

Stage 37 (embryo 61–65 days) FL: 35.78 mm. *Tail*: 12.8 cm. Maxillary process length: 16.38 mm and mandibular process length: 15.77 mm. The eyelids are opening and have been reduced to a narrow slit. The otic capsule is small. The forelimbs and hindlimbs are robust, and pigmentation expresses striking grey. The body has more intense pigmentation. The yolk is starting incorporation into the abdominal cavity (Figure 7e).

Stage 38 (embryo 65–69 days) FL: 35.85 mm. *Tail*: 13.3 cm. Maxillary process length: 14.65 mm, and mandibular process length:13.44 mm. The eyes are closed. The otic capsule is almost covering. The hindlimbs are more robust than forelimbs. About 50% of the yolk is incorporated into the abdominal cavity (Figure 7f).

Stage 39 (embryo 70–72 days) FL: 35.80 mm. *Tail*: 14.2 cm. Maxillary process length: 19.39 mm, and mandibular process length: 1510 mm. The eyes are completely closed. The auditory capsule is small. The forelimbs and hindlimbs are robust and pigmented. About 50% of the yolk is incorporated into the abdominal cavity of the embryo. The shell begins to break (Figure 7g).

Stage 40 (embryo 73 days) Weight: 9 g: full length 36 cm. *Tail*: 14.5 cm. Maxillary process length: 19.47 mm and mandibular process length: 18.73 mm. The forelimbs and hindlimbs are similar to juvenile pigmentation. Yolk completely incorporated into the abdominal cavity (Figure 7h).

4 | DISCUSSION

During the embryonic development, remarkable changes were evidenced in the shell, from the compaction of the fibers, the ordering of the same; the increase in the quantity of calcareous rosettes; however, one of the most notable changes in the shell was the thinning of the thickness of the calcareous layer both in the area of the poles and in the equator. The reduction in thickness could be due to the phenomena of intrinsic and extrinsic degradation. About intrinsic degradation, Packard and Packard (1989) pointed out that the egg yolk is an important calcium resource for the embryo, particularly in the second third of the incubation. However, in the last third, calcium would be mobilized from the shell. The process of calcium mobilization would reduce the thickness of the shell and increase its flexibility (Simoncini et al., 2014). The changes noticed in the egg shells, from the middle of the incubation period until hatching, correspond to the growth and development of the embryo and to bone maturation processes that require the incorporation of calcium (Oviedo-Rondon et al., 2008, Simoncini et al., 2014). The extrinsic degradation is another critical factor in the thinning of the shell, since the presence of microorganisms, water, and carbon dioxide in the nest material erodes the shell from the surface, deteriorating the ornamentation (Simoncini et al., 2014, Simoncini et al., 2019).

Some authors describe that eggs with a rigid shell improve the survival of the embryo and provide longer incubation periods (with slower development) than eggs with a flexible shell (Andrews, 2018). This was not evident in *S. merianae* since although the incubation period is prolonged, with slow embryonic development, the eggs presented flexible eggshells, this flexibility can be given by the greater proportion and the particular arrangement that both the fibers and rosettes have calcareous, providing strength and elasticity.

The rigidity of the shell is also related to the expansion of the allantoic chorion membrane, being substantially larger in the surface in eggs with rigid shells and reaching its highest degree of expansion in stages 30–35 (Andrews, 2018); however, this was not so evident in *S. merianae*, where the membrane expansion was rapid and reached its total coverage of the surface of the egg in the middle stage of development.

The embryonic development of Salvator merianae, takes 73 days to reach the final stage (Table 1). Summary of the stages embryonic of *S. merianae* reading incubation time and their main features.

Comparing development tables among different lizards may be difficult due to the incompatibility of criteria

TABLE 1 Summary of the stages embryonic development of *S. merianae*

Stages of embryonic development	Key features
Early stages	Incubation comprehending since the primitive streak, the curled body of the C-shape embryo until maxillary and mandibular the process has fused with frontal process and forelimb with plate digital.
Middle stages	It begins to delimit the scales, appears the eyelid, and also appears claws of toes and fingers cornification and initiation of the pigmentation.
Late stages	It begins to delimit the scales, appears the eyelid, and also appears claws of toes and fingers cornification and initiation of the pigmentation.

used by other authors. The differences mainly focus on *S. merianae* it's ancestral oviparous lizards, which at the time of post-oviposition occurs in the gastrula stage. Unlike most studies in other lizards, which are oviparous but with a degree of embryonic retention, which makes it difficult for the comparison of morphological characters and their moment of appearance in embryonic development. According to several authors, the description of embryonic stages could have differences in terms of chronology even if they have the same controlled incubation conditions, thus presenting congruences between the comparisons (Wise et al. 2009, Lima et al., 2018). Although in *S. merianae*, embryonic stages were recently described (Iungman et al., 2019), these consider different stages that are described in this article.

Particularly to *S. merianae*, the embryos presented nearly the development stage after oviposition that corresponds to 13–14 *Lacerta vivípara*, characterized by the formation of the primitive streak (Dufaure and Hubert 1961). Most Squamata lay their eggs at stage 26–33 (Andrews et al., 2000; Shine 1983). However, in phylogenetically related taxa, it has been reported that some lizards species retain their eggs until stage 22–24 *Paraedura pictus* (Gekkonidae; Noro et al., 2009) others until stage 26–26 *Calotes versicolor* (Dufaure and Hubert 1961) and in Polycrotides until stage 27 (Álvarez et al., 2005). This shows that the species has not established embryonic retention with relation to other lizards (Álvarez et al., 2005; Dufaure and Hubert 1961; Noro et al., 2009), with the ancestral oviparous condition being preserved as in turtles and birds (Crastz 1982; Yntema 1968). This study is the first contribution to embryology and the embryonic state in which the *S. merianae* egg is laid. Although there is a brief description of this species (Iungman et al., 2019), it is not specified about the oviductal transit or the first stages of development since they describe the development after 72 hr of incubation (stage 5).

The moment of the hatching of a species is an important factor to take into account the embryonic development. It is easy to compile some data on the hatching stage. The most lizard has presented a longer incubation period, for example, *Eublepharis macularius* (Wise et al., 2009), *Calotes versicolor* (Muthukkaruppan et al., 1970), *Podorcis murals*, *Podorcis viridis* (Dhouailly and Saxod 1974), and *Tropidurus torquatus* (Py-Daniel et al., 2017) finish the incubation period at stage 42. The longest hatching state was recorded for *Chamaleo lateralis* (Blanc 1974) and *Iguana iguana* (Muñoz et al., 2003) that finish the incubation period in stage 44. For *S. merianae*, the hatching stage was stage 40 (73 days of incubations), same that *Anolis sagrei*, *Lacerta agilis exigua*, and *Urosaurus ornatus* (Dufaure and Hubert 1961; Mathies and Andrews 1999). It seems that the number of stages of incubation that a species presents would not be related to external factors or to the moment in which the egg is laid if it is early or late, but rather it would be phylogenetic conditions of each species, conserving evolutionary characters.

Extrauterine *S. merianae* embryogenesis from day 1 of development was described using 14 states with typical morphological characters, corresponding to those used by Dufaure and Hubert (1961) which was also a reference to the development of other lizards (Lemus et al., 1981; Muthukkaruppan et al., 1970; Py-Daniel et al., 2017; Sanger et al., 2008; Wise et al., 2009). However, for better comparison, we based on external morphological characters; the embryos *S. merianae* developmental stages have been organized in chronological sequence and divided into early, middle, and late stages.

The number of stages of embryonic development in this study allowed us to compare *S. merianae* with other species of different taxa and observe similarities and differences between related groups. Variations in the appearance of both the scales and plaques as establishing the typical adult coloration were evident in the middle and later stages of development, as in most of the studied lizards (Py-Daniel et al., 2017; Wise et al., 2009).

The pharyngeal arches are an important feature to be highlighted in the comparison of structures in embryonic development (Py-Daniel et al., 2017). Some author has shown compared the number of pharyngeal arches present with the moment eyes pigmentation, a coincidence that is present in the pleurodont iguanids (Lemus et al., 1967; Lemus et al., 1981; Py-Daniel et al., 2017; Sanger et al., 2008). At this moment, five pharyngeal arches are visible in *S. merianae* (in E. 11) with optic placode are visible, five are distinctly visible with the advancement of eye pigmentation in *L. tenius* (Lemus et al., 1981). The pharyngeal arches in *L. tenius* (Lemus et al., 1981) remain visible for a longer period. These two correlated elements would be important to determine the period of ocular pigmentation, which usually occurs early in the ontogenetic development as occurs in *S. merianae*.

There are few know about the development of the genitals in reptiles. In the Squamata, the genital outline appears from the ventral side of the yolks of the hindlimbs (Gredler et al., 2015; Tschopp et al., 2014). We observed the same pattern in *S. merianae*, a proximal ventral bulge appears in the buds of the hindlimbs in stages 14 (early stages), coinciding with these authors. This condition that the genital primordium appears early in embryonic development could be related to the long incubation period that this species presents. The appearance of the external genitalia early in the ontogenetic

development was similar to that of the reptiles studied previously (Tschopp et al., 2014). This particular characteristic could be an ancestral condition of evolutionary origin.

In most groups of animals, the development of copulatory organs provides significant information on characters used by systematics (Arnold 1986). The appearance of the hemipenes occurs before gonadal development; even the gonadal outline begins in both sexes in a similar manner in stage 15 (Beck and Wade 2008; Raynaud and Pieau 1985). It was observed in *S. merianae* that the development of hemipenis occurs in stage 20, coinciding with what occurs in other reptiles (Arnold 1986; Beck and Wade 2008; Raynaud and Pieau 1985).

Limbs development is one of the most informative criteria used. For lizards, forelimbs buds usually develop before the hindlimbs buds (Lemus, 1967; Sanger et al., 2008; Noro et al., 2009; Wise et al., 2009; Gregorovicova et al., 2012; Khannoon 2015; Py-Daniel et al., 2017) and in other species, both forelimbs and hindlimbs develop concomitantly (Lemus and Duvauchelle 1966, Dufaure and Hubert, 1961; Muthukkaruppan et al., 1970; Mouden et al., 2000). Most of the studies were performed in species with embryonic retention, at the time of oviposition (stage 22–24 *Lacerta*, Dufaure and Hubert, 1961; stage 25–26 *Anolis sagrei* Sanger et al., 2008, and *Tropidurus torquatus* stage 28 Py-Daniel et al., 2017). Our results show that *S. merianae*, in stage 7, after oviposition, shows the forelimb bud before that the hindlimb bud. Thanks to these contributions, it is interpreted that in the overo lizard, as the complete development occurs outside the mother's uterus, the members begin to develop post-ovispotura. We can also confirm that the ectodermal outbreak begins first in the forelimb, and then the posterior one develops as in several species of iguanids such as *Liolaemus gravenhorstii*, *Anolis sagrei* (Lemus, 1967, Sanger et al., 2008)

The morphogenesis of the scales, the pigmentation, and the development of the color pattern are aging for the final phases of ontogenetic development (Py-Daniel et al., 2017). Interesting differences are observed in the comparisons between lizards, the development of the scales occurs at the beginning of the middle stages, from the limit of the dorsal, and caudal scales (E. 25). Taking into account other species, this event occurs relatively early than *E. macularis* (Stage 38). Another difference that we find is with *L. vivipara* that the coloration pattern first occurs in the scales of the extremities (Viets et al., 1994). In *S. merianae* at the end of the intermediate stages, in stage 29, the pigmentation begins initially extending from the dorsal region of the body to the ventral region thereof. In other groups, the pattern of formation is reserved, first occurring in the ventral region and then in the dorsal region (Ferguson 1985, 1987; Vieira et al., 2011). We can interpret that the differences found at the beginning of the pigmentation and the coloration pattern could be exclusive characters of each taxon. Comparative studies on the development of these lizards offer opportunities to investigate the evolution of basic biology in one of the largest and most basal radiations of the Squamata (Townsend et al., 2004; Conrad 2008). A minor detail is that the two species present in Argentina, *S. merianae* ("overa iguana") and *S. rufescens* ("red iguana"), traditionally exploited by native and rural communities (Donadio and Gallardo 1984; Norman 1987) they are currently in intense extraction in search of leather, most of which goes to the central countries like EE.UU., European Economic Community, Hong Kong, Japan (Fitzgerald et al., 1991).

Therefore, providing information relevant to its reproductive biology and ontogenetic development contributes to a complete overview of the general biology of this species as well as it allows us to develop plans for the proper management of captive breeding. Bearing in mind that the morphological events of the species reared in captivity, as in the case of this study, are consistent with the sequences established for other species of lizards.

ACKNOWLEDGMENTS

This study was supported by the 2012–2016 Scientific Programming, SEGCYT-UNNE PI-16F-011. Director: Lombardo, Daniel.

AUTHOR CONTRIBUTIONS

María Arrieta: Conceptualization; formal analysis; investigation; methodology; writing-original draft; writing-review and editing. **Gabriela Olea:** Conceptualization; formal analysis; investigation; methodology; writing-original draft; writing-review and editing. **Florencia Rodriguez:** Methodology; writing-review and editing.

ORCID

Gabriela Beatriz Olea https://orcid.org/0000-0002-2816-0263

Florencia Evelyn Rodríguez https://orcid.org/0000-0002-9967-8393

REFERENCES

Abdala, F., Lobo, F., & Scrocchi, G. (1996). Patterns of ossification in the skeleton of *Liolameus quilmes* (Iguania, Tropiduridae). *Amphibia-Reptilia*, *17*, 1–9. https://doi.org/10.1163/156853897X00323

Álvarez, B. B., Lions, M. L., & Calamante, C. (2005). Biología reproductiva y desarrollo del esqueleto de *Polychrus acutirostris* (Iguania: polichrotidae). *FACENA*, *21*, 3–27.

Andrews, R. M., Mathies, T., & Warner, D. A. (2000). Effect of incubation on morphology, growth, and survival of Juvenil *Sceloporus undulaus*. *Herptological Monographs*, *14*, 420–431.

Andrews, R. M. (2018). Changing perspectives on reptile eggs: One biologist's journey from demography to development. *Journal of Herpetology*, *52*(3), 243–251. https://doi.org/10.1670/17-050

Arias, F., & Lobo, F. (2006). Patrones de osificación en *Tupinambis merianae* y *Tupinambis rufescens* (squamata: teiidae) y patrones generales en squamata. *Cuadernos de herpetología.*, *20*(1), 3.23.

Arnold, E. N. (1986). Why copulatory organs provide so many useful taxonomic characters: the origin and maintenance of hemipenial differences in lacertid lizards (Reptilia: Lacertidae). *Biological Journal of the Linnean Society*, *29*(4), 263–281.

Ávila Pires, T. C. S. (1995). *Lizards of the Brazilian Amazonia (Reptilia: Squamata)* (p. 299). Zoologische Verhandelingen. National Natuurhistorisch Museum, Leiden, Holland.

Beaupre, S. B., Jacobson, E. R., Lilliywhite, H. B., & Zamudio, K. (2004). *Guidelines for use of live amphibians and reptiles in field and laboratory research* (2nd ed.). Lawrence, Kansas: Herpetological Animal Care and Use Committee of the American Society of Ichthyologists and Herpetologists.

Beck, L . A., & Wade, J. (2008). Steroid receptor expression in the developing copulatory system of the green anole lizard (Anolis carolinensis). *General and Comparative Endocrinology*, *157*(1), 70–74.

Beggs, K., Young, J., & Georges, A. (2000). Ageing the eggs and embryos of the pig-nosed turtle, *Carettochelys insculpta* (Chelonia: Carettochelydidae), from northern Australia. *Canadian Journal of Zoology.*, *78*, 373–392. https://doi.org/10.1139/z99-214

Blanc, F. (1974). Table de développement de *Chamaeleo lateralis* gray, 1831. *Annales D'Embryologie et de Morphogenese.*, *7*, 99–115.

Boughner, J. C., Buchtová, M., Fu, K., Dewert, V., Hallgrímsson, B., & Richman, J. M. (2007). Embryonic development in *Python sebae* I: Staging criteria and macroscopic skeletal morphogenesis of the head and limbs. *Zoology*, *110*, 212–230. https://doi.org/10.1016/j.zool.2007.01.005

Conrad, J. L. (2008). Phylogeny and systematic of Squamata (Reptilia) based on morphology. *Bulletin of the Aminal Museum of Natural History*, *310*, 1–182.

Crastz, F. (1982). Embryological stages of the marine turtle *Lepidochelys olivacea* (Eschscholtz). *Revista Biologica Tropical*, *30*, 113–120.

Dhouailly, D., & Saxod, R. (1974). Les stades du developpement de *Lacerta muralis* Laurent entre la ponte et l'éclosion. *Bulletin de la Société Zoologique de France*, *99*, 489–494.

Donadio, O., & Gallardo, J. M. (1984). Biología y conservación de las especies del género *Tupinambis* (Squamata, Sauria, Teiidae) en la Republica Argentina. *Revista del Museo Argentino de Ciencias Naturales Bernardino Rivadavia Zoologia*, *13*(11), 117–127.

Dufaure, J. P., & Hubert, J. (1961). Table de developpement *du lezard vivipare*: *Lacerta (Zootoca) vivipara* jacquin. *Archives D Anatomie Microscopique Et De Morphologie Experimentale*, *50* (3), 309.

Duméril, A. M. C., & Bibron, G. (1839). *Erpétologie Générale on Histoire Naturelle Complète des Reptiles* (Vol. 5, p. 871). Paris: Roret/Fain et Thunot.

Ferguson, M. W. J. (1985). Reproductive biology and embryology of the crocodilians. In C. Gans, F. Billet, & P. F. A. Maderson (Eds.), *Biology of the reptilian* (pp. 329–491). New York: John Wiley and Sons.

Ferguson MWJ. 1987. Post-laying stages of embryonic development in crocodilians: In: Webb, G.J.W., Manolis, S.C. And Whitehead, PJ. *Wildlife management: Crocodiles and alligators*. Chipping Norton: Surrey Beatty & Sons. 427-444.

Fernández, M. S., Simoncini, M. S., & Dyke, G. (2013). Irregularly calcified eggs and eggshells of *Caiman latirostris* (Alligatoridae: Crocodylia). *Naturwissenschaften*, *100*(5), 451–457.

Fitzgerald, L. A., Chani, J. M., & Donadio, O. E. (1991). Tupinambis lizards in Argentina: Implementing management of a traditionally exploited resource. In *Neotropical wildlife use and conservation* (pp. 303–316). Chicago, IL. J. Robinson, K. Redford (Eds.), Neotropical Wildlife: Use and Conservation, University of Chicago Press.

Fitzgerald, L. A., Porini, G., & Lichtschein, V. (1994). El manejo de *Tupinambis* en Argentina: Historia, estado actual y perspectivas futuras. *Interciencia*, *19*(4), 166–170.

Garcia Valdez, M. V., Chamut, S. N., Valdez Jaen, G., Arce, O. E., & Manes, M. E. (2011). Dynamics of ovarian follicles in *Tupinambis merianae* lizards. *Acta Herpetologica*, *6*(2), 303–313.

Gredler, M. L., Sanger, T. J., & Cohn, M. J. (2015). Development of the cloaca, hemipenes, and hemiclitores in the green anole, *Anolis carolinensis*. *Sexual Development*, *9*, 21–33.

Greenbaum, E. B., & Carr, J. L. (2002). Staging criteria for embryos of the spiny softshell turtle, *Apalone spinifera* (Testudines: Trionychidae). *Journal of Morphology*, *254*, 272–291. https://doi.org/10.1002/jmor.10036

Gregorovicova, M., Zahradnicek, O., Tucker, A. S., Velensky, P., & Horacek, I. (2012). Embryonic development of the monitor lizard, *Varanus indicus*. *Amphibia-Reptilia.*, *33*, 451–468.

Günther, A. (1871). Description of a New Species of Tejus:(Tejus rufescens) from Mendoza. *The Proceedings of the Zoological Society of London*, *1871*, 541–543.

Hamburger, V., & Hamilton, H. L. (1992). A series of normal stages in the development of the chick embryo. *Developmental Dynamics*, *195*, 231–272.

Harvey, M. B., Ugueto, G. N., & Gutberlet, J. R. (2012). Review of Teiidae morphology with a revised taxonomy and phylogeny of the Teiidae (Lepidosauria: Squamata). *Zootaxa*, *3459*, 1–156.

Iungman, J. L., Molinero, M. N., Simoncini, M. S., & Piña, C. I. (2019). Embryological development of *Salvator merianae* (Squamata: Teiidae). *Genesis*, *57*(4), 23–28.

Iungman, J., Piña, C. I., & Siroski, P. (2008). Embryological development of *Caiman latirostris* (Crocodylia: Alligatoridae). *Genesis*, *46*, 401–417. https://doi.org/10.1002/dvg.20413

Kamal, A. M., Hammouda, H. G., & Mokhtar, F. M. (1970). The development of the osteocraniium of the Egyptian cobra: IN. The Embryonic Osteocranium. *Acta Zoologica*, *970*, 1–17. https://doi.org/10.1111/j.1463-6395.1970.tb00415.x

Kamal, A. M., & Hammouda, H. G. (1965). The development of the skull of *Psammophis sibilans*. I. The development of the chondrochranium. *Journal of Morphology*, *116*, 197–245. https://doi.org/10.1002/jmor.1051160205

Khannoon, E. R. (2015). Developmental stages of the climbing gecko *Tarentola annularis* with special reference to the claws,

pad lamellae, and subdigital setae. *Journal of Experimental Zoology Part B: Molecular and Developmental Evolution*, *324B*, 450–464.

Lemus, D., & Duvauchelle, R. (1966). Desarrollo intrauterino de *Lioluemus tenuis tenuis*. Contribución al Estudio del Desarrollo embriológico de Reptiles. *Biológica*, *39*, 80–89.

Lemus, D., Illanems, J., Fuenzaliday, M., de la Vega, P., & García, M. (1981). Comparative analysis of the development of the lizard, *Liolaemus tenuis tenuis* II. A series of normal post-laying stages in embryonic development. *Journal of Morphology*, *169*, 337–349. https://doi.org/10.1002/jmor.1051690307

Lemus, D. (1967). Tabla de desarrollo de la lagartija vivipara *Lioluemus gravenhorsti* (Reptilia: Squamata.:Iguanidae). *Biológica*, *40*, 39–61.

Lima, F. C., Py-Daniel, T. R., Sartori, M. R., Abe, A. S., dos Santos, P. O., Freitas, L. M., … Sebben, A. (2018). Developmental staging table of the green iguana. *Acta zoológica*, *100*, 232–244. https://doi.org/10.1111/azo.12245

Lima, F. C., Vieira, L. G., Santos, A. L., Silva-Junior, L. M., SBS, D. S., Silva, J. M., & Malvázio, A. (2012). Ontogeny of the shell bones of embryos of *Podocmenis unifilis*. *The Anatomical Record*, *294*, 621–632. https://doi.org/10.1002/ar.21359

Lobo, F., Abdala, F., & Scrocchi, G. (1995). Desarrollo del esqueleto de *Liolaemus scapularis* (Iguania, Tropiduridae). *Bollutein Museo Regionale di Scienze Naturali, Torino*, *13*(1), 77–104.

Magnusson, W. E., & Taylor, J. A. (1980). A description of developmental stages in *Crocodylus porosus*, for use in adding eggs in the field. *Australian Wildlife Research*, *7*, 479–485. https://doi.org/10.1071/WR9800479

Manes, M. E., Ibañez, M. A., & Manlla, A. (2003). Factores físicos y conductas de nidificación de lagartos *Tupinambis merianae* en cautiverio. *Revista Argentina de Producción Animal*, *23*(2), 119–126.

Manes, M. E., Noriega, T., Campos Casal, F., & Apichela, S. (2007). Ovarian changes during the reproductive cycle of the *Tupinambis merianae* lizard raised in a temperate environment. *Cuadernos de herpetología*, *21*(1), 21–29.

Mathies, T., & Andrews, R. M. (1999). Determinants of embryonic stage at oviposition in the lizard *Urosaurus ornatus*. *Physiological and Biochemical Zoology*, *72*, 645–655. https://doi.org/10.1086/316707

Melo de Almeida, H., Sousa, R. P., Oliveira Bezerra, D., Gomes Olivindo, R. F., Diniz, A. N., Oliveira, S. C., … Martins de Carvalho, M. A. (2015). Greater rhea (*Rhea americana*) external morphology at different stages of embryonic and fetal development. *Animal Reproduction Science*, *162*, 43–51.

Mouden, E. E., Bons, J., Pieau, C., Renous, S., Znari, M., & Boumezzough, A. (2000). Table de d eveloppement embryonnaire d'un l ezard agamid e, *Agama impalearis* Boettger, 1874. *Annales des Sciences Naturelles-Zoologie et Biologie Animale*, *21*, 93–115.

Muñoz, E. M., Ortega, A. M., Bock, B. C., & Paéz, V. P. (2003). Demografía y ecología de anidación de la iguana verde, *Iguana iguana* (Squamata: Iguanidae), en dos poblaciones explotadas en la Depresión Momposina, Colombia. *Revista de Biología Tropical*, *51*(1).229–240.

Murray, J. R., Varian-Ramos, C. W., Weich, Z. S., & Saha, M. S. (2013). Embryological Stanging of the zebra finch, *Taeniopygia guttata*. *Journal of Morphology*, *274*, 1090–1110. https://doi.org/10.1002/jmor.20165

Muthukkaruppan, V. R., Kanakambika, P., Manickavel, V., & Veeraraghavan, K. (1970). Analysis of the development of the lizard, *Calotes versicolor*. I. A series of normal stages in the embryonic development. *Journal of Morphology*, *130*(4), 479–489. https://doi.org/10.1002/jmor.1051300407

Noriega, T., Fogliatto, O., Mignola, L., & Manes, M. E. (1996). Ciclo biológico y patrones de comportamiento en una población de iguanas overas *Tupinambis teguixin* (L). (Sauria: Teiidae). Adapatada al cautiverio. *Revista agronómica Noroeste Argentina*, *XXVIII*(1-4), 109–127.

Norman, D. R. (1987). Man and tegu lizards in eastern. Paraguay. *Biological Conservation*, *41*, 39–56. https://doi.org/10.1016/0006-3207(87)90046-2

Noro, M., Uejima, A., Abe, G., Manabe, M., & Tamura, K. (2009). Normal developmental stages of the Madagascar ground gecko *Paroedura pictus* with special reference to limb morphogenesis. *Developmental Dynamics*, *238*, 100–109. https://doi.org/10.1002/dvdy.21828

Olea, G. B., & Sandoval, M. T. (2012). Embryonic development of *Columba livia* (Aves: Columbiformes) from an altricial-precocial perspective. *Revista Colombiana de Ciencias Pecuarias*, *25*(1), 3–13.

Oviedo-Rondón, E. O,, Oviedo-Rondón, J., Wineland, M. J., Christensen, V. L., Mozdziak, P. Z., Koci, M. D., Funderburk, S. L.V., Ort, D.T., & Mann, K.M.(2008). Broiler embryo bone development is influenced by incubator temperature, oxygen concentration and eggshell conductance at the plateau stage in oxygen consumption. *British Poultry Science*, *49*, 666–676.

Packard, M. J., & Packard, G. C. (1989). Mobilization of calcium phosphorus and magnesium by embryonic alligators (*Alligator mississippiensis*). *American Journal of Physiology*, *257*, 1541–1547.

Parker, W. K. (1879). On the structure and development of the skull in the common snake *Tropidonotus natrix*. *Philosophical Transactions of the Royal Society of London*, *169*, 385–417.

Pike, D. A., Andrews, R. M., & Du, W. G. (2012). Eggshell morphology and gekkotan life-history evolution. *Evolutionary Ecology*, *26*(4), 847–861.

Py-Daniel, T. R., De-Lima, A. K., Lima, F. C., Pic-Taylor, A., Pires-Junior, O. R., & Sebben, A. (2017). A staging table of post-ovipositional development for the south American collared lizard *Tropidurus torquatus* (Squamata: Tropiduridae). *The Anatomical Record*, *300*, 277–290. https://doi.org/10.1002/ar.23500

Renous-Lécuru, S., Rimblot-Baly, F., Fretey, J., & Pieau, C. (1989). Caractéristiques du développement embryonnaire de la tortue luth, *Dermochelys coriacea* (Vandelli, 1761). *Annales des Sciences Naturelles Zoologie et Biologie Animale*, *10*, 197–229.

Rieppel, O. (1993). Studies on skeletonformation in reptiles. II. *Chamaeleo hoehnelii* (Squamata: Chamaeleoninae), with comments on the homology of carpal and tarsal bo nes. *Herpetologica*, *49*, 66–78.

Rodríguez, F. E., Sandoval, M. T., Álvarez, B. B., & Lombardo, D. M. (2018). Comparative study of prenatal development between *Myotis albescens* (Chiroptera: Vespertilionidae) and *Eumops patagonicus* (Chiroptera: Molossidae): The chorionic vesicle and extraembryonic membranes considerations. *The Anatomical Record*, *301*(9), 1527–1543.

Sanger, T. J., Losos, J. B., & Gibson-Brown, J. J. (2008). A developmental staging series for the lizard genus *Anolis*: A new system for the integration of evolution, development, and ecology. *Journal of Morphology*, *269*, 129–137. https://doi.org/10.1002/jmor.1056

Shine, R. (1983). Reptilian reproductive modes: The oviparity-viviparity continuum herpetologica. *Herpetologica.*, *39*(1), 1–8.

Simoncini, M. S., Fernandez, M., & Iungman, J. (2014). Structural changes in eggshells of *Caiman latirostris*. *Revista Mexicana de Biodiversidad*, *85*(1), 78–83.

Simoncini, M. S., Leiva, P. M., Piña, C. I., & Cruz, F. B. (2019). Influence of temperature variation on incubation period, hatching success, sex ratio, and phenotypes in *Caiman latirostris*. *Journal of Experimental Zoology Part A: Ecological and Integrative Physiology*, *331*(5), 299–307.

Townsend, T. M., Larson, A., Louis, E., & Macey, J. R. (2004). Molecular phylogenetics of Squamata: The position of snakes, amphisbaenians, and dibamids, and the root of the squamate tree. *Systematic Biology.*, *53*(5), 735–757.

Tracy, C. R., Packard, G. C., & Packard, M. J. (1978). Water relations of chelonian eggs. *Physiological Zoology*, *51*, 378–386.

Vieira, L. G., Lima, F. C., Santos, A. L., Mendoça, S. H., Moura, L. R., Iasbeck, J. R., & Sebben, A. (2011). Description of embryonic stages in *Melanosuchus Niger* (Spix, 1825) (Crocodylia: Alligatoridae). *Journal of Morphological Sciences*, *28*(1), 11–22.

Wink, C. S., Elsey, R. M., & Bouvier, M. (1990). Porosity of eggshells from wild and captive, pen-raised alligators (*Alligator mississippiensis*). *Journal of Morphology*, *203*, 3539.

Wise, P. A., Vickaryous, M. K., & Russell, A. P. (2009). An embryonic staging table for in Ovo development of *Eublepharis macularius*, the leopard gecko. *The Anatomical Record*, *292*, 1198–1212. https://doi.org/10.1002/ar.20945

Yanoski, A. A., & Mercolli, C. (1995). Incubación artificial de huevos de iguana overa (*Tupinambis Teguixin*) (Sauria: Teiidae). *Archivos de Zootecnia*, *44*, 379–389.

Yanoskiy, A. A., & Mercolli, C. (1991). Temperaturas internas y frecuencias de muda en crías de *Tupinambis teguixin* (Reptilia: teiidae) bajo condiciones controladas. *Cuadernos de Herpetología*, *6*(4),. 23–26.

Yntema, C. L. (1968). A series of stages in the embryonic development of *Chelydra serpentina*. *Journal of Morphology*, *125*, 219–251.

How to cite this article: Arrieta MB, Olea GB, Rodríguez FE, Lombardo DM. Ultrastructure of eggshell and embryological development of *Salvator merianae* (Squamata: Teiidae). *Anat Rec*. 2021;304:1420–1438. https://doi.org/10.1002/ar.24546